Conference materials
UDC 537.9
DOI: https://doi.org/10.18721/JPM.161.111

Low-field magnetization features of superconducting tapes with strong pinning anisotropy

V.V. Guryev [1]✉, A.V. Irodova [1], N.K. Chumakov [1], S.V. Shavkin [1]

[1] National Research Centre "Kurchatov Institute", Moscow, Russia

✉ Gurev_VV@nrcki.ru

Abstract. The electrodynamic behavior of II-type superconductors is determined by the physics of the vortex matter, for which the superconducting material is the medium of existence. It is noteworthy that for all practical superconductors this medium is both anisotropic and inhomogeneous. On the basis of data on the degree of inhomogeneity and anisotropy, some features of magnetization in low external field, comparable to self-field, can be explained. Namely: 1) an anomalous shift of the central magnetization peak, and 2) the fishtail shape in inclined magnetic fields. In this paper, we present an experimental study of the low-field magnetization of Nb-Ti tapes. The degree of anisotropy was varied by heat treatment of the original cold-rolled tape and by slicing the samples along and across the rolling direction. The obtained results are discussed in comparison with the features of the magnetization loops of other practical superconductors.

Keywords: vortex matter, magnetization, fishtail, pinning anisotropy

Citation: Guryev V.V., Irodova A.V., Chumakov N.K., Shavkin S.V., Low-field magnetization features of superconducting tapes with strong pinning anisotropy, St. Petersburg State Polytechnical University Journal: Physics and Mathematics. 16 (1.1) (2023) 67–73. DOI: https://doi.org/10.18721/JPM.161.111

Материалы конференции
УДК 537.9
DOI: https://doi.org/10.18721/JPM.161.111

Особенности низкополевой намагниченности сверхпроводящих лент с сильной анизотропией пиннинга

В.В. Гурьев [1]✉, А.В. Иродова [1], Н.К. Чумаков [1], С.В. Шавкин [1]

[1] Национальный исследовательский центр «Курчатовский институт», Москва, Россия

✉ Gurev_VV@nrcki.ru

Аннотация. Электродинамика сверхпроводников II рода определяется физикой ансамбля вихрей, для которых сверхпроводящий материал является средой существования. Примечательно, что для всех технических сверхпроводников эта среда одновременно анизотропна и неоднородна. На основании данных о степени неоднородности и анизотропии можно объяснить некоторые особенности намагниченности в слабом внешнем поле, сравнимом с собственным. А именно: 1) аномальный сдвиг центрального пика намагниченности, и 2) форма «fishtail» в наклонных магнитных полях. В этой статье мы представляем экспериментальное исследование низкополевой намагниченности сверхпроводящих Nb-Ti лент. Степень анизотропии варьировалась с помощью термической обработки исходной холоднокатаной ленты и путем нарезки образцов вдоль и поперек направления прокатки. Полученные результаты обсуждаются в сравнении с особенностями петель намагничивания других технических сверхпроводников.

Ключевые слова: ансамбль вихрей, намагниченность, fishtail, анизотропия пиннинга

Ссылка при цитировании: Гурьев В.В., Иродова А.В., Чумаков Н.К., Шавкин С.В., Особенности низкополевой намагниченности сверхпроводящих лент с сильной анизотропией пиннинга // Научно-технические ведомости СПбГПУ: Физико математические науки. 2023. Т. 16. № 1.1. С. 67–73. DOI: https://doi.org/10.18721/JPM.161.111

Introduction

Quite a long time has passed from the prediction by A.A. Abrikosov of magnetic flux quantization in type II superconductors [1] to the acceptance by the scientific community of vortex matter as a new state of condensed matter. It turned out that in practically important cases anisotropy plays an essential role in the physics of vortex matter [2]. It is customary to distinguish between external and internal causes of anisotropy. Internal with respect to vortex matter or intrinsic anisotropy is the anisotropy of the thermodynamic critical fields H_{c1} and H_{c2}, which leads through the coherence length ξ and the penetration length λ to the anisotropy of the vortices spatial dimensions. This type of anisotropy is typical for HTS, in which the structural unit cell itself is strongly anisotropic [3]. The external anisotropy is due to the anisotropy of the pinning center morphology, which takes place in all practical superconductors, both in HTS and in traditional ones such as Nb_3Sn and Nb-Ti. Vortices, unlike particles, are essentially elongated objects. Therefore, generally one should distinguish between anisotropy with respect to the direction of the magnetic field B, and anisotropy with respect to the direction of the driving force $\boldsymbol{F} = [\boldsymbol{j} \times \boldsymbol{B}]$, which, for a fixed direction of the magnetic field, is determined by the direction of the transport current density $\boldsymbol{j}$ [4].

This is a fairly exhaustive classification of anisotropy types. Note that even in an isotropic superconductor a tensor relationship between current density and electric field has been predicted [4]. Therefore, the mismatch of the directions of these vectors cannot serve as a criterion for the presence of anisotropy.

The distinction between the causes of anisotropy becomes important when interpreting the features in the low-field parts of the magnetization curves $M(H)$, which arise in planar superconductors in tilted magnetic fields. Magnetization measurements have been proven to be a useful tool for estimating critical current density [5]. Models have been developed and widely used to estimate the in-plane anisotropy of the critical current in perpendicular magnetic field [6, 7], which is a special case of anisotropy with respect to the driving force, and to estimate the angular dependence of the critical current in the configuration of the maximum driving force (the vectors of the magnetic field and current density are always perpendicular to each other) [8, 9]. However, with rare exceptions, such as [10], the low-field part of magnetization is not analyzed. This is mainly due to the fact that the analysis is difficult, since the combined influence of the self-field and anisotropy leads to a non-uniform current distribution over the cross-section [11, 12]. At the same time, there are intriguing effects, such as a low-field fishtail in tilted magnetic fields [13, 14] and an anomalous shift of the central magnetization peak [15, 16, 17]. The latter effect is especially important, because, on the one hand, it allows one to estimate the degree of granularity [18]; on the other hand, its presence may indicate that the models mentioned above for critical current estimating are not applicable [15].

In this paper, we present the studies of the low-field magnetization of a 10 μm thick Nb-Ti tape heat-treated at 385 °C/25 h in comparison with the original cold-rolled one. In cold-rolled single-phase β-Nb-Ti tape, the pinning centers are the grain boundaries. The heat treatment led to the precipitation of 6% volume α-Ti particles, acting as strong pinning centers [19]. In accordance with previous transport measurements, the presence of α-Ti particles significantly increases the volume pinning force and reduces its anisotropy [20].

Materials and Methods

For magnetic studies 4 samples were selected, sliced along (RD-samples) and across the rolling (TD-samples) (Table 1). Slicing samples with an optimal length-to-width ratio can significantly reduce the edge effect in tilted magnetic fields [8]. The parameters of our measuring system are close to those, used in [8], and therefore the optimal aspect ratio is also about 5. Previously, samples prepared in a similar way were investigated by the transport method in a liquid helium environment at 4.2 K [4, 20, 21]. Table 1 provides descriptions, dimensions, and transport method data for the tested samples. In the series of samples from № 1 to № 4, the value of the critical current density measured at 1 T in perpendicular geometry (the external magnetic field $\boldsymbol{H}$ is co-directed with the normal of the tape $\boldsymbol{n}$: $\boldsymbol{H} \| \boldsymbol{n}$) increases. At the same time, the ratio of the critical current densities when the field, lies in the plane of the tape ($\boldsymbol{H} \perp \boldsymbol{n}$) to the current density in the perpendicular geometry ($\boldsymbol{H} \| \boldsymbol{n}$) decreases. This ratio can serve as a rough estimate of the anisotropy degree in the maximum driving force configuration. The critical currents were measured not only at 1 T, but in a much wider range of magnetic fields up to the upper critical field. The obtained field dependencies were approximated by the frequently used scaling law [22]:

$$j_c H = C\left(\frac{H}{H_{irr}}\right)^p \left(1 - \frac{H}{H_{irr}}\right)^q, \tag{1}$$

where j_c is the critical current density, H is the applied magnetic field, H_{irr} is the irreversibility field $\mu_0 H_{irr} \approx 10.6$ T [23, 24], C, p, q are fitting parameters. For magnetic fields $\mu_0 H < 1$ T, p is the key fitting parameter. This parameter does not exceed unity and shows how fast the critical current density increases with decreasing magnetic field: $j_c \sim H^{p-1}$. These values are also given in Table 1.

Table 1

Description of samples and their current carrying capacity, obtained by transport measurements

Sample	Condition	Slicing	Size, mm × mm	j_c(1T, $\boldsymbol{H} \| \boldsymbol{n}$), kA/mm^2	$j_c(\boldsymbol{H} \perp \boldsymbol{n})/j_c(\boldsymbol{H} \| \boldsymbol{n})$, at 1T	p, $\boldsymbol{H} \perp \boldsymbol{n}$
№ 1	cold-worked	TD	11.7 × 2.1	0.24	13	0.8
№ 2		RD	11.4 × 1.9	0.58	6	0.7
№ 3	heat-treated	TD	11.6 × 2.1	0.83	6	0.6
№ 4		RD	11.3 × 1.9	1.33	4	0.4

The magnetization curves were measured with the Vibrating Sample Magnetometer “LakeShore 7400 series VSM System” with the magnet field of up to 1 T. The sample oscillated perpendicular to the magnetic field lines. Each magnetization curve was recorded at different orientations of the sample to the magnetic field, at certain rotating angle around the axis passing through the central line of the sample. A component of the magnetization vector parallel to the external magnetic field direction was recorded. The measurements were carried out at 5 K in a helium gas medium. The experiment consisted of the following steps. The magnetization was measured on a sample cooled in a zero magnetic field. Then the system was heated to 20 K (far above the critical temperature of Nb-Ti ~ 9 K), the orientation angle of the sample was changed, and the sample was again cooled down in a zero magnetic field.

Results and Discussion

Figure 1 shows the magnetization loops of the tested samples at 5 K and at different orientations of the magnetic field. Usually plane samples are examined in perpendicular geometry, so it is convenient to begin discussions with this orientation. Remarkable that for transverse samples № 1 and № 3 an anomalous shift of the central magnetization peak is observed, while it is not the case for longitudinal samples № 2 and № 4. This effect was considered in detail in [15] and is related to the inhomogeneous penetration of the flux into the sample due to variations in the tape thickness in the transverse direction. Please note that the scale on the vertical axes is different. The width of the hysteresis loop increases for samples from 1 to 4, which corresponds to known trends for such heat treatment [25, 26, 27]. This is also consistent with transport measurements (Table 1) since the loop width ΔM is proportional to the critical current density j_c [7]:

$$\Delta M = \frac{j_{cl} w}{2}\left(1 - \frac{w}{3l}\frac{j_{cw}}{j_{cl}}\right), \quad (2)$$

where l and w are the length and width of the rectangular sample; j_{cl} and j_{cw} are the critical current density along the length and width, respectively. Formula (2) can be used for quantitative estimates (Table 2). Clearly, if an anomalous shift of the central magnetization peak is observed, then (2) gives an overestimated value of the critical current density. Here two things must be noted. First, transport measurements were carried out at 4.2 K while magnetic measurements — at 5 K, so the critical current should be lower in the latter case. Second, the electric field criterion for magnetic measurements is lower than for transport measurements [8]. Consequently, the estimate of the critical current, obtained from magnetic measurements, should be lower than for transport measurements, which is not the case for transverse samples № 1 and № 3. This confirms the conclusions of the work [15] that the anomalous central peak shift indicates an inhomogeneous flux penetration. This leads to the fact that Formula (2), obtained in the framework of the critical state model, gives an overestimated value compared to transport measurements.

Table 2

Comparison of transport measurements and magnetic estimates at 1 T

Sample	Slicing	Anomalous central peak shift	j_c (1 T, 4.2 K), kA/mm^2 transport	j_c (1 T, 5 K), kA/mm^2 magnetization
№ 1	TD	Yes	0.24	0.27
№ 2	RD	No	0.58	0.48
№ 3	TD	Yes	0.83	0.84
№ 4	RD	No	1.33	1.16

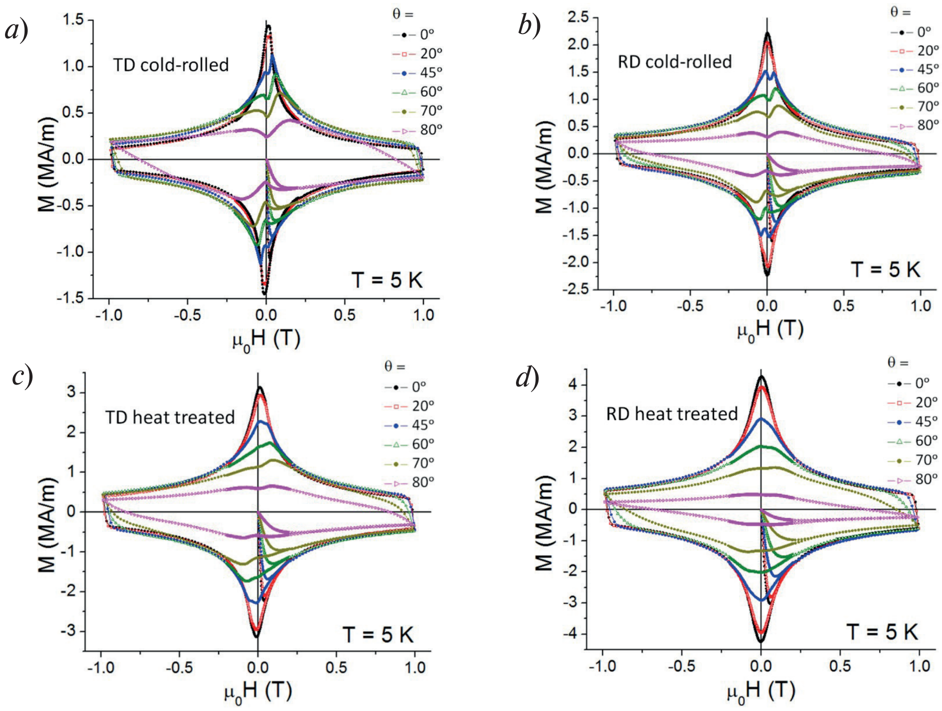

Fig. 1. Magnetization curves for samples № 1 (a), № 2 (b), № 3 (c) and № 4 (d). The angle between the normal to the tape and the magnetic field is indicated in the legend

As for tilted magnetic fields, there are several theoretical works, predicting interesting phenomena [28, 29, 30]. A low-field fishtail for superconductors with anisotropic pinning has been predicted [14]. The essence of this effect is as follows. When the self-field of screening currents is comparable to the external field, there are locations in the cross-section of the sample, where the direction of magnetic induction deviates significantly from the direction of the external magnetic field. If the critical current density has a pronounced anisotropy, then this leads to a sharply non-uniform distribution of the current over the cross section and may lead to a non-monotonic dependence of the total magnetization on the external field. This effect was actually observed in inclined magnetic fields on cold-rolled Nb-Ti tape [13]. Figure 1 shows the evolution of this effect at different angles of the magnetic field for samples with different degrees of anisotropy (Table 1). The low-field fishtail effect occurs on stationary hysteresis loops, when the direction of the external magnetic field differs from normal direction ($\theta \neq 0°$) and manifests itself initially as a violation of the symmetry of the central peak (see loops at $\theta = 20°$ in Figures 1, *a* and 1, *b*) with subsequent splitting of the central peak into two smaller ones (at angles $\theta = 45°, 60°, 70°, 80°$ in Figures 1, *a* and 1, *b*). Moreover, these features appear only on the stationary hysteresis magnetization curve, while the virgin curves are free of any features. This is an important fact, because it allows one to distinguish between intrinsic and external anisotropy. Intrinsic anisotropy is characterized by the appearance of an additional peak on the virgin curve and the absence of any features on the stationary hysteresis curve [31, 32]. When a sample with intrinsic anisotropy is magnetized in an inclined magnetic field, it is energetically favorable for the vortices to turn, so that the dimensions of the vortex become smaller. If the pinning is sufficiently weak and the rotation of the vortices is not hindered, then this appears as a double peak on the virgin branch of the magnetization curve: the first peak corresponds to the penetration of the vortices into the whole sample cross section, and the second corresponds to the full rotation of vortices in the direction of the external field [33]. In terms of the generalized critical state model, this corresponds to successive penetration of magnetic field components [34].

Qualitatively, with a decrease in the anisotropy degree the severity of the low-field fishtail effect reduces with almost complete disappearance for sample №4 with a minimum degree of anisotropy. It is interesting to compare the hysteretic loops for samples №2 and №3, the anisotropy of which has the similar value (Table 1), but the fishtail effect for sample №3 is much less pronounced. Such a significant difference may seem especially strange, since the critical current, and hence the self-field of sample №3, is higher than of sample №2, which means that the effect, associated with the curvature of magnetic lines by the self-field, should be more pronounced. However, it turns out that not only the ratio $j_c(\boldsymbol{H}\perp\boldsymbol{n})/j_c(\boldsymbol{H}\|\boldsymbol{n})$ is important for the occurrence of the low-field fishtail effect, but also the details of the critical current angular dependence. It was shown [21] that the critical current angular dependence of the Nb-Ti tape is well described by the two-parametric dependence:

$$j_c(\theta) = j_c(90°)\sqrt{\frac{(k^L\cos\theta)^2 + (\sin\theta)^2}{(k^U\cos\theta)^2 + (\sin\theta)^2}}, \tag{3}$$

where θ is the angle between the tape normal $\boldsymbol{n}$ and the magnetic field $\boldsymbol{H}$, k^L and k^U — the parameters of the angular dependence.

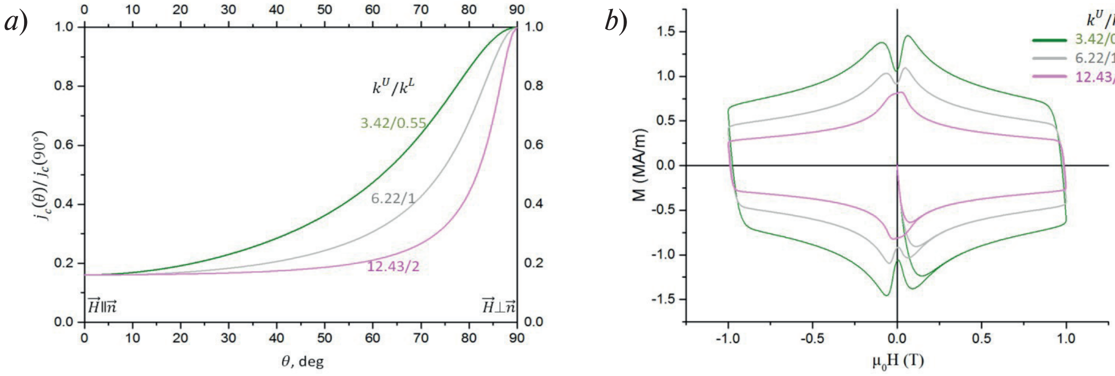

Fig. 2. Model angular dependencies with a different values of the parameters k^U and k^L at a constant ratio k^U/k^L (*a*). Corresponding simulated magnetization curves at $\theta = 70$ °(*b*)

From (3) it follows that $j_c(\boldsymbol{H}\perp\boldsymbol{n})/j_c(\boldsymbol{H}\|\boldsymbol{n}) = j_c(90°)/j_c(0°) = k^U/k^L$. Thus, the details of the angular dependencies are described by different sets of the parameters (Fig. 2). Using the angular dependence (3), the magnetization loops of a long flat sample with a width-to-thickness ratio $w/t = 10$ were calculated using the program, developed in [13]. The results are shown in Figure 2. For the same ratio $j_c(\boldsymbol{H}\perp\boldsymbol{n})/j_c(\boldsymbol{H}\|\boldsymbol{n})$, the low-field fishtail can have a different degree of severity, depending on the sharpness of the peak near $\theta = 90°$.

Conclusion

The low-field fishtail effect has been experimentally studied on samples with different degrees of external anisotropy. In contrast to intrinsically anisotropic superconductors, the magnetization curves of Nb-Ti samples in tilted magnetic fields do not show peculiarities on the virgin magnetization curve, while features are observed on the stationary hysteresis loops. Increasing the degree of anisotropy enhances the low-field fishtail effect. In addition, the manifestation of the low-field fishtail effect is sensitive to the details of the critical current angular dependence.

An anomalous shift in the central magnetization peak was observed for the transverse samples. It is shown that the estimation of the critical current density over the width of the magnetization loop, performed within the framework of the critical state model, yields overestimated values compared to the transport measurements.

Acknowledgments

The work was supported by NRC "Kurchatov Institute". The work was partially performed on the equipment of the resource center Electrophysics of the NRC "Kurchatov Institute".

REFERENCES

1. **Abrikosov A.A.,** The magnetic properties of superconducting alloys, Journal of Physics and Chemistry of Solids. 2 (3) (1957) 199–208.

2. **Blatter G., Feigel'man M.V., Geshkenbein V.B., Larkin A.I., Vinokur V.M.,** Vortices in high-temperature superconductors, Reviews of Modern Physics. 66 (1125) (1994).

3. **Vlasko-Vlasov V.K., Glatz A., Koshelev A.E., Welp U., Kwok W.K.,** Anisotropic superconductors in tilted magnetic fields, Phys. Rev. B. 91 (224505) (2015).

4. **Klimenko E.Yu., Shavkin S.V., Volkov P.V.,** Anisotropic pinning in macroscopic electrodynamics of superconductors, J. Exp. Theor. Phys. 85 (1997) 573–587.

5. **Caplin A.D., Cohen L.F., Perkins G.K., Zhukov A.A.,** The electric field within high temperature superconductors: mapping the E-J-B surface, Supercond. Sci. Technol. 7 (412) (1994).

6. **Gyorgy E.M., van Dover R.B., Jackson K.A., Schneemeyer L.F., Waszczak J.V.,** Anisotropic critical currents in $Ba_2YCu_3O_7$, analyzed using an extended Bean model, Appl. Phys. Lett. 55 (283) (1989).

7. **Sauerzopf F.M., Wiesinger H.P., Weber H.W.,** Anisotropic current flow and demagnetization corrections in the Bean model, Cryogenics. 30(7), 650–655 (1990).

8. **Hengstberger F., Eisterer M., Weber H.W.,** Magnetic measurement of the critical current anisotropy in coated conductors, Supercond. Sci. Technol. 24 (045002) (2011).

9. **Thompson J.R., Sinclair J.W., Christen D.K., Zhang Y., Zuev Y.L., Cantoni C., Chen Y., Selvamanickam V.,** Field, temperature, and angle dependent critical current density $j_c(H, T, \theta)$ in coated conductors, obtained via contact-free methods, Supercond. Sci. Technol. 23 (014002) (2010).

10. **Kapolka M., Pardo E.,** 3D modelling of macroscopic force-free effects in superconducting thin films and rectangular prisms, Supercond. Sci. Technol. 32 (054001) (2019).

11. **Mikitik G.P.,** Critical states in thin planar type-II superconductors in a perpendicular or inclined magnetic field (Review), Low Temperature Physics. 36 (13) (2010).

12. **Pardo E., Vojenciak M., Gomory F., Souc L.,** Low-magnetic-field dependence and anisotropy of the critical current density in coated conductors, Supercond. Sci. Technol. 24 (065007) (2011).

13. **Guryev V., Shavkin S., Kruglov V., Chumakov N., Emelyanov A.,** Magnetization of a superconducting Nb-Ti tape with anisotropic current-carrying capacity in an inclined magnetic field, AIP Conference Proceedings. 2163 (020004) (2019).

14. **Babich I.M., Mikitik G.P.,** On the nature of the fishtail effect in the magnetic hysteresis loop of high-*T* c-superconductors, Jetp. Lett. 64 (1996) 586–591.

15. **Shavkin S.V., Guryev V.V., Chumakov N.K., Irodova A.V., Kruglov V.S.,** Anomalous magnetization central peak shift of Nb-Ti tapes with high in-plane critical current anisotropy, J. Supercond. Nov. Magn. 35 (2022) 2119–2125.

16. **Palau A., Puig T., Obradors X., Pardo E., Navau C., Sanchez A., Usoskin A., Freyhardt H.C., Fernandez L., Holzapfel B., Feenstra R.,** Simultaneous inductive determination of grain and intergrain critical current densities of $YBa_2Cu_3O_{7-x}$ coated conductors, Appl. Phys. Lett. 84 (230) (2004).

17. **Johansen T.H., Shantsev D.V., Koblischka M.R., Galperin Y.M., Nalevka P., Jirsa M.,** The low-field peak in magnetization loops of uniform and granular superconductors in perpendicular magnetic fields, Physica C. P3(341–348) (2000) 1443–1444.

18. **Bonura M., Cayado P., Konstantopoulou K., Alessandrini M., Senatore C.,** Heating-induced performance degradation of $REBa_2Cu_3O_{7-x}$ coated conductors: An oxygen out diffusion scenario with two activation energies, ACS Appl. Electron. Mater. 4 (3) (2022) 1318–1326.

19. **Shavkin S., Guryev V., Kruglov V., Ovcharov A., Likhachev I., Vasiliev A., Veligzhanin A., Zubavichus Y.,** Features of microstructure and magnetic flux dynamics in superconducting Nb-Ti tapes with strong anisotropic pinning. EPJ Web of Conferences. 185 (08007) (2018).

20. **Guryev V., Shavkin S., Kruglov V.,** Guided vortex motion in dilute strong pinning environment: Models and experiment, Physica C. 599(13540802021) (2022).

21. **Guryev V.V., Shavkin S.V., Kruglov V.S.,** Method for critical current angular dependencies analysis of superconducting tapes, J. Phys.: Conf. Ser. 2103(012096) (2021).

22. **Dew-Hughes D.,** Flux pinning mechanisms in type II superconductors, Phil. Mag. 30 (2) (1974).

23. **Guryev V., Shavkin S., Kruglov V.,** Inhomogeneity and irreversibility field of superconducting Nb-Ti tapes, EPJ Web of Conferences. 185 (08004) (2018).

24. **Guryev V.V., Shavkin S.V., Kruglov V.S.,** Irreversibility field and anisotropic δl pinning in type II superconductors, J. Phys.: Conf. Ser. 1697 (012202) (2020).

25. **Baker C., Sutton J.,** Correlation of superconducting and metallurgical properties of a Ti-20 at.% Nb alloy, Philosophical Magazine, 19(1969) 1223–1255.

26. **Matsushita T., Kupfer H.,** Enhancement of the superconducting critical current from saturation in Nb-Ti wire. I, Journal of Applied Physics. 63 (5048) (1988).

27. **Kupfer H., Matsushita T.,** Superconducting critical current of Nb-Ti wire with anisotropic defect structure. II, Journal of Applied Physics. 63 (5060) (1988).

28. **Huang Chen-Guang, Liu Jun.,** Magnetic and mechanical properties of a finite thickness superconducting strip with a cavity in oblique magnetic fields, Journal of Applied Physics. 121 (023905) (2017).

29. **Pompeo N., Silva E.,** Analysis of the measurements of anisotropic AC vortex resistivity in tilted magnetic fields, IEEE Tranactions on Applied Supercond. 28 (2) (2018).

30. **Yokoji H., Kato M.,** Structures of vortices in a superconductor under a tilted magnetic field, J. Phys.: Conf. Ser. 1975 (012001) (2021).

31. **Voloshin I.F., Kalinov A.V., Fisher L.M., Derevyanko S.A., Yampol'ski V.A.,** A new type of peak effect in the magnetization of anisotropic superconductors, Jetp Lett. 73 (2001) 285–288.

32. **Bugoslavsky Yu.V., Ivanov A.L., Minakov A.A., Vasyurin S.I.,** Fishtails and anisotropy in underdoped LaSrCuO single crystals, Physica C. 233(1-2) 67–76.

33. **Buzdin A.I., Simonov A.Yu.,** Magnetization of anisotropic superconductors in the tilted magnetic field, Physica C. 175 (1991) 143–155.

34. **Romero-Salazar C., Perez-Rodriguez F.,** Critical state of anisotropic hard superconductors, Supercond. Sci. Technol. 16 (2003) 1273–1281.

THE AUTHORS

GURYEV Valentin V.
Gurev_VV@nrcki.ru
ORCID: 0000-0003-4946-2559

IRODOVA Alla V.
Irodova_AV@nrcki.ru

CHUMAKOV Nikolai K.
Chumakov_NK@nrcki.ru

SHAVKIN Sergey V.
Shavkin_SV@nrcki.ru

Received 17.10.2022. Approved after reviewing 22.11.2022. Accepted 22.11.2022.